

Thermal behavior of cement matrix with high-volume mineral admixtures at early hydration age

Mo Liwu, Deng Min *

College of Materials Science and Engineering, Nanjing University of Technology, Nanjing 210009, China

Received 3 November 2005; accepted 13 July 2006

Abstract

Thermal cracks that usually occur in mass concrete are closely related to the thermal behavior of cement matrix, such as heat liberation, temperature rise and thermal shrinkage. Cement pastes added with large-volume mineral admixtures that are usually used for thermal controlling were cast into well-sealed plastic cylinder and covered by heat insulation materials to simulate the pseudo-adiabatic condition of mass concrete. The deformation and temperature rise of cement specimens under the heat insulation condition have been examined at early hydration age. Results show that with addition of fly ash, coal gangue and blast furnace slag the heat liberation and peak temperature of cement paste decrease, while its total shrinkage increases.

There is no shrinkage but expansion of the pastes during the temperature rise process, which may be ascribed to the complete compensation of the shrinkage by thermal dilation of the pastes. The thermal dilation coefficient (TDC) of cement paste changes drastically with the hydration duration, and it is also related to the addition of mineral admixtures.

© 2006 Elsevier Ltd. All rights reserved.

Keywords: Admixture; Hydration; Thermal analysis; Shrinkage

1. Introduction

Shrinkage of concrete under restraining condition may induce tensile stress leading to cracks [1,2], which is of great concern to the durability of concrete structures. Noticeably, shrinkage of cement matrix, including autogenous shrinkage, drying shrinkage, carbonation shrinkage and thermal shrinkage, contributes mostly to the total shrinkage of concrete, being crucial factors of the shrinkage cracking. Moreover, due to the low tensile strength and large shrinkage of cement matrix at the early hydration age, the cracking potentiality is very high. Accordingly, much research work has been focused on the early-age shrinkage, trying to ascertain the magnitude of the shrinkage and develop corresponding preventive measures [3–5].

Thermal shrinkage is considered as the main cause of cracking in mass concrete, in which the peak temperature usually exceeds 60 °C due to significant heat liberation during cement hydration and poor heat conductivity of concrete [6]. Thermal shrinkage of cement matrix is hindered not only by the external restraint caused by groundwork or old concrete, but also by the internal restraint caused by thermal mismatch between aggregate and cement matrix due to their different thermal expansion coefficients. Therefore, the internal stress may be generated. Accurate estimation of the thermal behavior of cement matrix, such as heat liberation, temperature variation and thermal shrinkage, is a prerequisite to evaluating the thermal stress. In addition, since the

Table 1
Physical properties of cement

Initial setting time/min	Final setting time/min	Specific surface area/ m ² /kg	7d Compressive strength/MPa	28d Compressive strength/MPa
122	160	379	30.7	62.3

* Corresponding author. Tel.: +86 025 83587232; fax: +86 025 83221984.

E-mail addresses: andymoliwu@sohu.com (M. Liwu), dengmin@njut.edu.cn (D. Min).

Table 2
Chemical composition of cement and mineral admixtures

Raw materials	Chemical composition									Total
	SiO ₂	Al ₂ O ₃	Fe ₂ O ₃	CaO	MgO	SO ₃	Na ₂ O	K ₂ O	Loss/%	
Cement	21.74	5.06	3.56	66.6	0.88	0.81	0.05	0.55	1.26	99.25
Fly ash	49.96	33.02	4.52	6.09	1.17	0.62	0.66	0.98	1.68	98.70
Slag	32.43	14.99	0.43	36.50	11.00	0.06	–	–	–1.27	99.96
Coal gangue	55.50	18.15	5.42	3.38	1.23	0.64	0.64	1.67	13.32	99.95

thermal shrinkage, ε_{th} , is proportional to the thermal dilation coefficient (TDC) of the cement matrix: $\varepsilon_{th} = TDC \times \Delta T$, the development of thermal stress is strongly affected by the TDC. Evidently, TDC is indispensable for better understanding the thermal behavior of cement matrix.

The mineral admixtures (fly ash, coal gangue and blast furnace slag) have been used as an effective measure to control the thermal crack for its effects on reducing heat liberation and lowering temperature rise of cement materials [7–10]. The dosage of mineral admixture added is becoming higher and higher, even being 60% in roller compacted concrete [11]. However, the thermal behavior of cement matrix with high-volume mineral admixtures at early hydration age has been investigated by few work.

In the present work, to investigate the thermal behavior of cement matrix with high-volume mineral admixtures at early age, 40% mineral admixtures by mass were added as partial replacement of cement and the cement pastes were cast into a well-sealed plastic cylinder in which no water was transferred to the environment, the drying shrinkage being prevented. In addition, pseudo-adiabatic condition of mass concrete was simulated by covering the specimens with heat insulation materials.

2. Experimental

2.1. Materials

2.1.1. Cement

Portland cement produced by Jiangsu-Onada Cement Corp., Nanjing, China was used. Physical properties and chemical composition of this cement are shown in Tables 1 and 2.

2.1.2. Mineral admixtures

Coal gangue used is a waste residue separated from coal mine. The gangue was calcined at 1200 °C for 1 h, and then crushed into fine particles with specific surface area of 350 m²/kg. Its chemical

composition is shown in Table 2. Type I fly ash produced by Huaneng Power Plant, Nanjing and blast furnace slag from Nanjing New Materials Corp. were also used. The chemical compositions of the two additives are shown in Table 2.

2.2. Experimental procedure

2.2.1. Strain transducer

Type-VWS strain transducer made by GN Instrument Corp., Nanjing was used. The vibrating modulus of the strain transducer, F , is closely related to the length of strain transducer, varying with the length change of the transducer brought about by deformation of cement paste. F was recorded directly by a collecting apparatus. The temperature of the paste was measured using a thermocouple included in the transducer. The temperature detection ranged from – 25 °C to 70 °C. The strain of specimens was calculated by Eq. (1).

$$\varepsilon = k\Delta F + b\Delta T \quad (1)$$

where, k is a constant of the strain transducer; ΔF is the change of vibrating modulus; b is temperature correction coefficient of the strain transducer; ΔT is the temperature variation.

2.2.2. Preparation of specimens

Mix proportions of the cement paste specimens are given in Table 3. The content of mineral admixtures is 40% by mass of the total cementitious materials.

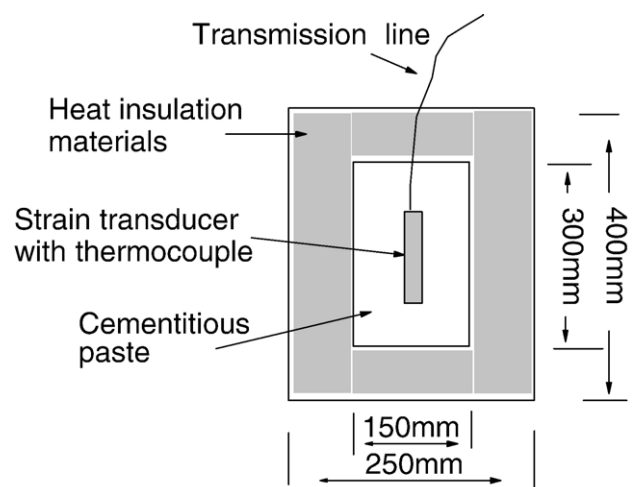


Fig. 1. Schematic representation of the apparatus.

Table 3
Mix proportion of the specimens

Mix ID	Mix proportion/%				
	w/c	Cement	Coal gangue	Fly ash	Blast furnace slag
C	0.30	100	–	–	–
CG	0.30	60	40	–	–
CF	0.30	60	–	40	–
CGF	0.30	60	30	10	–
CGB	0.30	60	30	–	10
CGBF	0.30	60	20	10	10

Two PVC cylinders with size of $\phi 150 \text{ mm} \times 300 \text{ mm}$ and $\phi 250 \text{ mm} \times 400 \text{ mm}$ were prepared and their bottoms were sealed with PVC boards. The smaller cylinder was set into the bigger one, and the space between the two cylinders was filled up with heat insulation materials made of rock wool with thermal conductivity of 0.058 W/m K (Fig. 1). The cement and mineral admixtures were mixed in a pan mixer, and then mixed with water until a consistent mixture was obtained. The consistent paste was cast into the inner cylinder in two layers, and the strain transducer was embedded into the center of the paste during casting. The paste was consolidated by vibration of 30 s. The strain transducer should be kept at the center of the paste vertically during the casting process (Fig. 1).

After that, the paste was sealed by a $150 \text{ mm} \times 150 \text{ mm}$ PVC board with a hole at the center for the pass of transmission line and the board was covered with heat insulation materials. Lastly, the bigger cylinder was sealed by a $250 \text{ mm} \times 250 \text{ mm}$ PVC board and then transferred to a curing room at 25°C . All the preparation process should be completed within 20 min. As

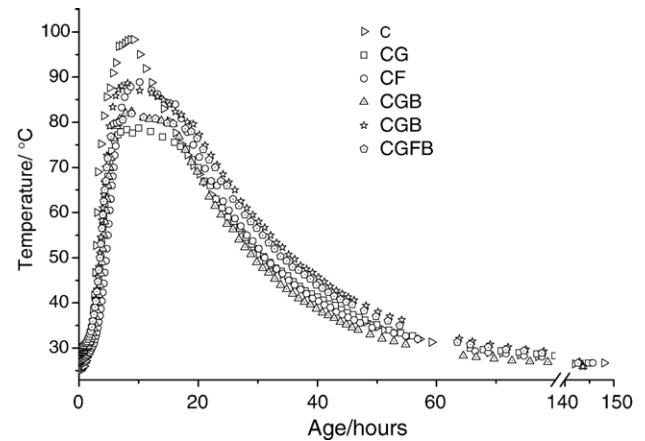


Fig. 3. Fitting curves of temperature versus hydration age.

the cement paste was well sealed, there was no loss of moisture for the paste, and thus the drying shrinkage due to water evaporation could be ignored.

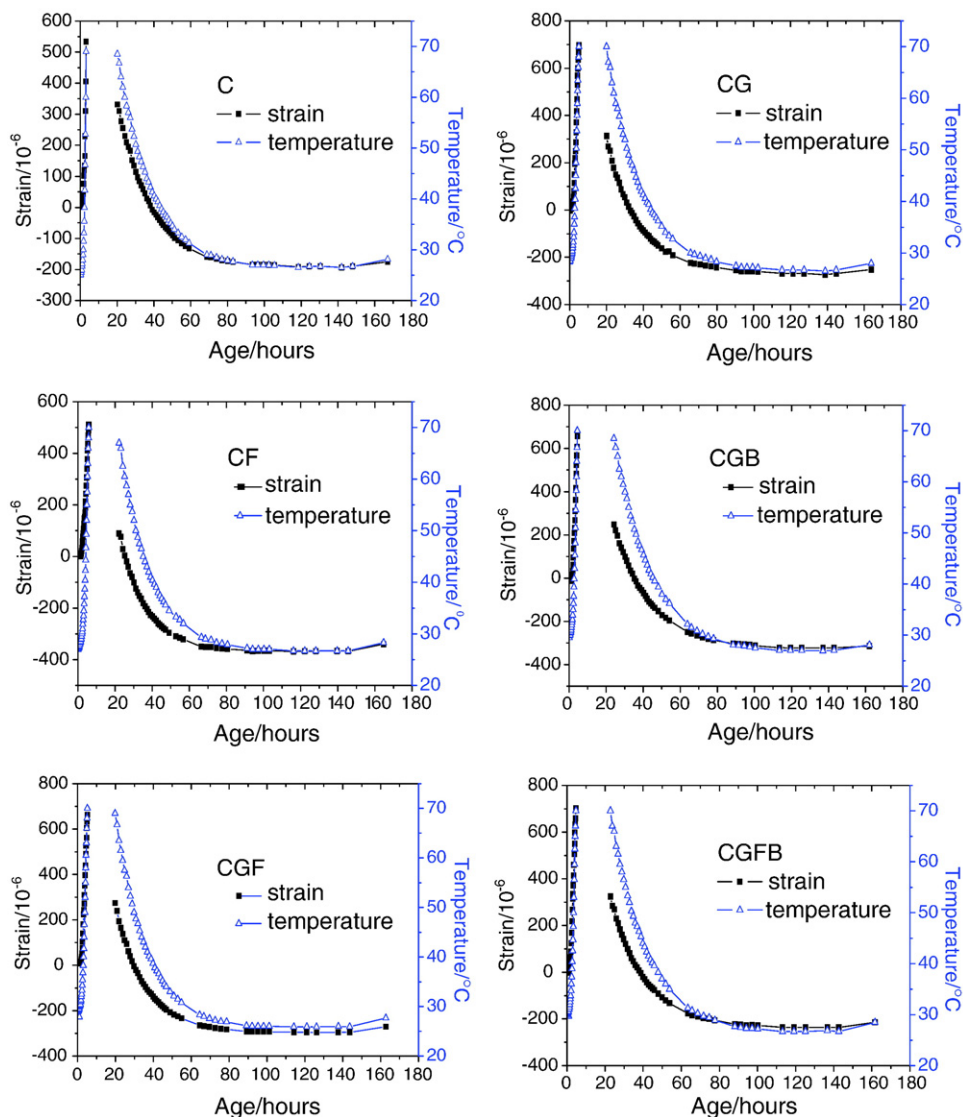


Fig. 2. Strain and temperature of specimens versus hydration age.

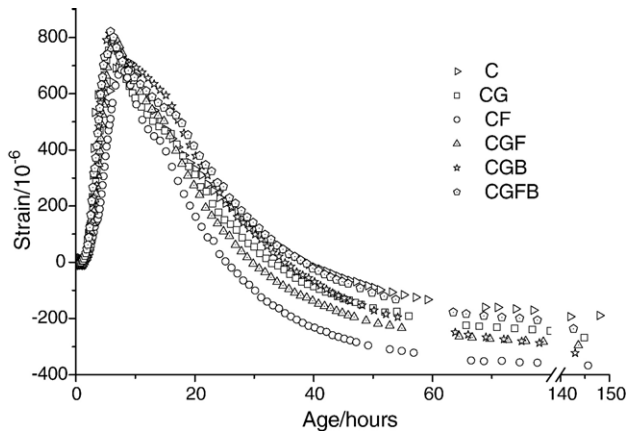


Fig. 4. Fitting curves of strain versus hydration age.

2.3. Determination of temperature and strain of specimens

The vibrating modulus and temperature of the strain transducer at different curing age were recorded by a collecting apparatus connected to the transducer by the transmission line.

3. Results and discussion

3.1. Variations of strain and temperature of specimens

The strain and temperature of specimens at continuous hydration age are shown in Fig. 2. It is to be noted that the temperatures of all the specimens rise to 70 °C in several hours after casting. For specimen C it takes only 4 h to reach 70 °C, while for other pastes it takes longer time due to the lower heat liberation rate of hydration caused by addition of mineral admixtures. Since the temperature measuring range of the thermocouple is −25 °C–70 °C, the temperature exceeding 70 °C cannot be detected, and thus the corresponding strain cannot be calculated yet.

During the temperature ascension process, none of the specimens shows any shrinkage which always occurs in normal situation (Fig. 2). Instead, the pastes expand at early age until the temperature declines. This may be caused by thermal dilation of the cement paste due to the significant and fast temperature rise under the heat insulation condition, though the autogenous shrinkage occurs simultaneously. Some researchers [12–14] suggested that the autogenous shrinkage could be compensated partly by the thermal dilation derived from the hydration heat of cement. In consideration of the thermal insulation condition, it is conceivable that the autogenous shrinkage is completely compensated by thermal dilation for the present case.

The peak temperature can be obtained by fitting the data with Gauss peak function (as shown in Eq. (2)), all the correlation coefficients of fitting curves being above 0.93. The corresponding strain can be calculated according to Eq. (1). The fitting curves are shown in Figs. 3 and 4.

$$T = T_0 + \frac{A}{w\sqrt{\pi i/2}} \exp\left(-2\frac{(x-x_c)^2}{w^2}\right) \quad (2)$$

where, T and x represent the temperature and the hydration age of cement paste respectively; A , w , x_c and are the fitting parameters built during the fitting process.

The fitting results are shown in Table 4. The peak temperature of specimen C is 98.9 °C reached in 7.8 h after casting, while the peak temperatures of others are lower and the corresponding ages are longer, indicating that the addition of mineral admixtures results in decreasing the heat liberation of hydration and delaying the occurrence of peak temperature, which is favorable for the thermal shrinkage controlling. However, the shrinkages (difference between the maximum expansion and the ultimate shrinkage) during the temperature decline process of the pastes added with mineral admixtures are greater than that for neat cement paste C.

During the cooling stage of the pastes, the thermal shrinkage may contribute mostly to the total shrinkage of the pastes, though the autogenous shrinkage takes place at the same time. The thermal shrinkages of the specimens with mineral admixtures are increased to different extent in comparison with specimen C, which may be attributed to the difference in the thermal dilation characteristics of these pastes, such as the thermal dilation coefficients.

3.2. Thermal dilation coefficient (TDC)

3.2.1. TDC of specimens during temperature rise stage

As shown in Fig. 5, for each specimen there are two inflexion points indicated by arrows in the curve of strain against temperature during the temperature rise stage, occurring at age of around 2 h and 3 h, which may result from the physico-chemical and structural evolution of cement paste during continuous stiffening process and appears to be relevant to initial and final settings.

Three stages are defined by the two inflexion points. The curve at each stage was fitted by linear regression separately. The slope of the linear fits was TDC (Table 5). At the first stage, which is from the casting completion to the first inflexion point, the cement paste is still fresh and does not possess enough strength to force the embedded strain transducer to generate equivalent deformation simultaneously. The strain of transducer may be much less than the actual strain of specimens. So the TDC of the paste specimens obtained at this stage may be much lower than its actual value which has been reported to be $90 \times 10^{-6}/^{\circ}\text{C}$ [12]. Free water, which is not chemically bonded during hydration and has a higher TDC of $207 \times 10^{-6}/^{\circ}\text{C}$ than cement materials [15], may contribute mainly to the high TDC of cement paste at the initial hydration age.

Table 4

Peak temperature, corresponding hydration duration and total shrinkage of specimens

Mix ID	C	CG	CF	CGF	CGB	CGFB
Peak temperature/°C	98.9	78.5	87.9	82.5	88.1	83.4
Corresponding hydration duration/h	7.8	10.4	10.5	10.2	9.5	11.6
Total shrinkage/ $\times 10^{-6}$	894	1035	1024	1062	1127	1036

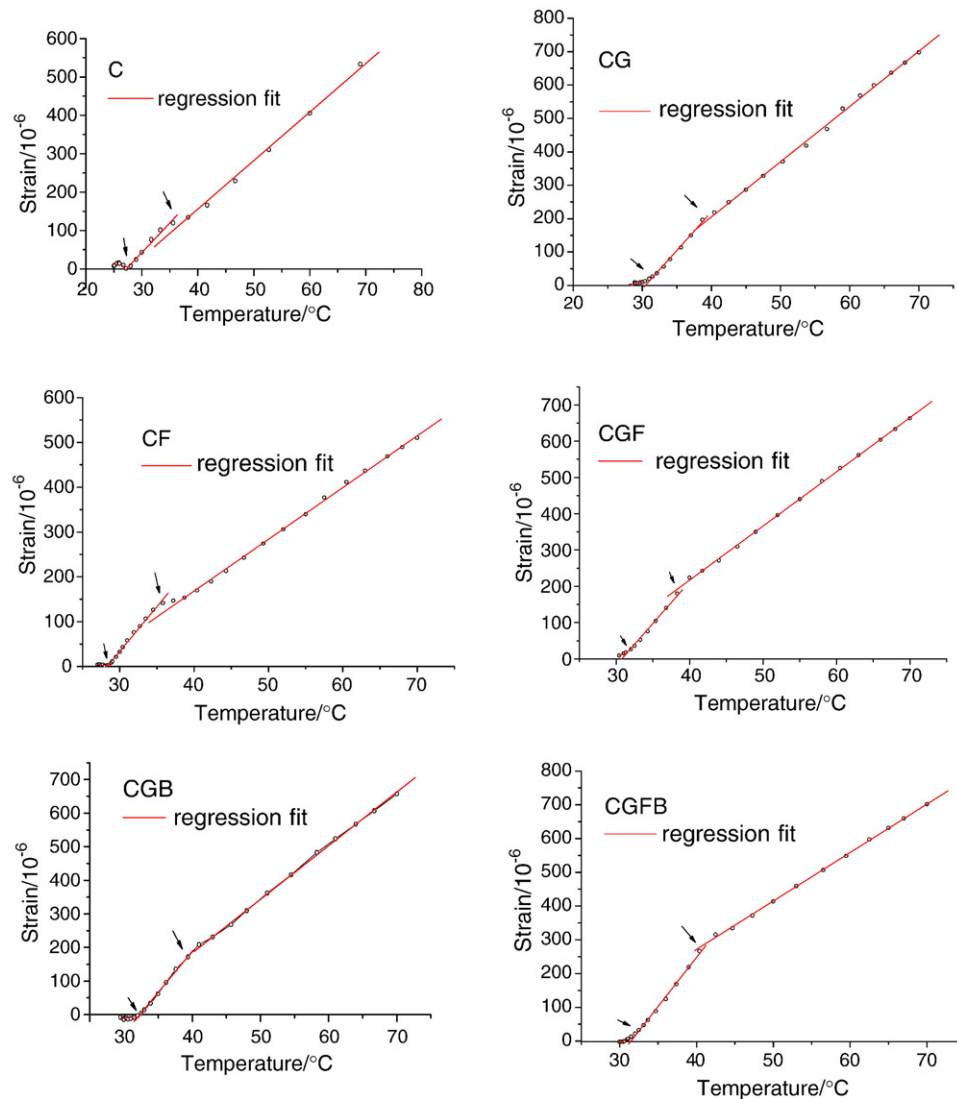


Fig. 5. Plots of strain against temperature during temperature rise stage; arrows indicate the inflexion points.

At the second stage (stage between the two inflexion points) and the last stage (from the second inflexion point to peak temperature), with continuous hydration, the hydration products become denser and a rigid skeleton with adequate strength is formed. Hence, the strain transducer deforms simultaneously and equivalently with the pastes. As a consequence of quick consumption of the free water during hydration, the TDC of the

specimens drop sharply by about $10 \times 10^{-6}/^{\circ}\text{C}$ from the second stage to the third stage except specimen C which only drops by $2 \times 10^{-6}/^{\circ}\text{C}$ (Table 5). This may be due to less reduction of free water for specimen C at the third stage. Ahmed Loukili [12] who has determined TDC based on hydrostatic weighing method suggested that the rapid decrease of TDC is a result of phase transformation of materials from liquid state to a

Table 5
TDC of specimens at the early hydration age

Mix ID	Before the first inflexion point		Between the two inflexion points		From the second inflexion point to peak temperature		Cooling stage	
	TDC $\times 10^{-6}/^{\circ}\text{C}$	R^2	TDC $\times 10^{-6}/^{\circ}\text{C}$	R^2	TDC $\times 10^{-6}/^{\circ}\text{C}$	R^2	TDC $\times 10^{-6}/^{\circ}\text{C}$	R^2
C	—	—	15.419	0.988	13.127	0.999	12.573	0.999
CG	8.179	0.977	24.193	0.999	16.534	0.999	13.028	0.999
CF	9.539	0.951	19.482	0.996	11.542	0.999	11.038	0.998
CGB	8.802	0.936	22.348	0.992	15.981	0.999	13.555	0.999
CGF	5.792	0.902	25.305	0.999	15.024	0.999	12.908	0.999
CGFB	16.169	0.981	29.607	0.999	14.553	0.999	12.761	0.999

R^2 represents the correlation coefficient of linear fit.

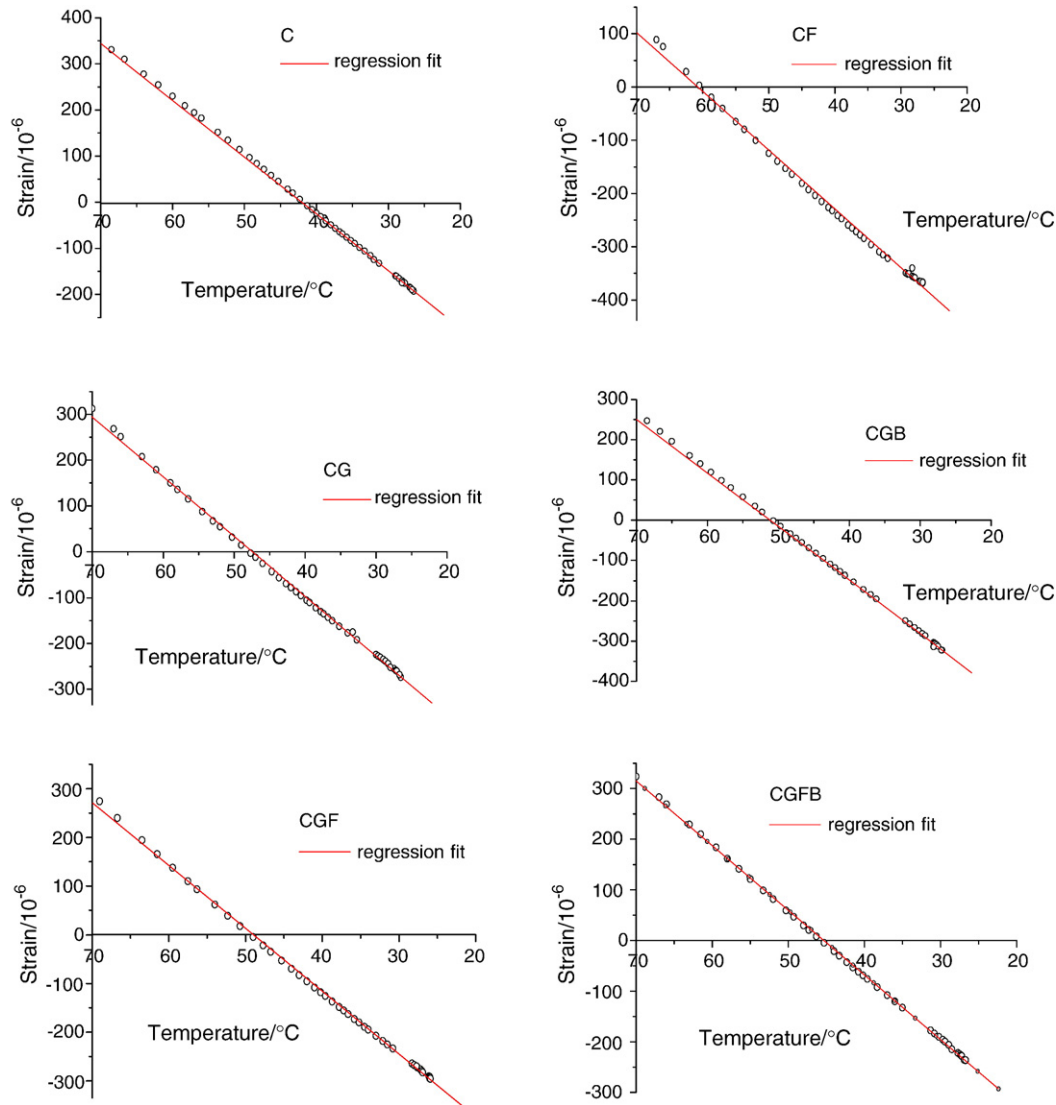


Fig. 6. Plots of strain against temperature during cooling stage.

hardened state involving reaction of large volume of free water. It is shown from Table 5 that TDC of the specimens with different high-volume mineral admixtures is not identical at the same stage, and changes more markedly compared to neat cement paste, owing to the different hydration rate and different properties of hydration products due to addition of different mineral admixtures [15]. As shown in Table 5, addition of admixtures may cause increase of TDC of the pastes, especially at the second stage.

3.2.2. TDC of specimens during the cooling stage

The plots of strain against temperature during cooling stage are shown in Fig. 6. TDC of the specimens during cooling stage is given in Table 5. With continuous hydration, the amount of free water continues to be reduced and the hydration products accumulate, giving rise to a decrease in TDC. However, the decrease extent is smaller compared to previous stage, the largest being only about $3.5 \times 10^{-6}/^{\circ}\text{C}$ for CG, and the smallest being about $0.5 \times 10^{-6}/^{\circ}\text{C}$ for C and CF. It has been reported that beside the reduction of free water, the structural properties

of hydration products such as density play an important role in the thermal dilation of cement pastes [16].

4. Conclusions

1. Under the heat insulation condition, the total deformation of the specimen tested is expansion rather than shrinkage during the temperature rise process, which implies that the autogenous shrinkage is completely compensated by thermal dilation of the cement pastes owing to significant temperature increase.
2. Addition of mineral admixtures reduces the total heat liberation and lowers the peak temperature of cement pastes, which is favorable for thermal crack prevention. However, the total shrinkage increases during the cooling stage, which seems to counteract the aforementioned thermal crack prevention.
3. The TDC of the tested cement pastes changes with continuous hydration, especially at the initial hydration age. The value of TDC is higher for the cement matrix with

high-volume mineral admixtures compared to neat cement paste, which may be ascribed to the different hydration rate of cementitious materials and the different characteristics of hydration products.

Acknowledgement

Special appreciations are given to Mr. Steven Martindale who works in Geotechnical and Pavement Design in California, USA and Professor Yuguiyu, Nanjing University of Technology, China for their review of this paper. The authors would also like to thank Mr. Chenchun of the Nanjing University of Technology who assisted much in the experiment.

References

- [1] M.J. Kawamura, Internal stress and microcracks formation caused by drying shrinkage in hardened cement paste, *J. Am. Ceram. Soc.* 61 (7–8) (1978) 281.
- [2] F. Sancier, M. Pigeon, Durability of new-to-old concrete bonding, *Proceedings of the ACI International Conference on Evaluation and Rehabilitation of Concrete Structures and Innovations in Design*, Hong Kong, 1991, pp. 689–705.
- [3] E. Holt, M. Leivo, Cracking risks associated with early age shrinkage, *Cem. Concr. Res.* 26 (2004) 521–530.
- [4] B. Person, Experimental studies on shrinkage of high-performance concrete, *Cem. Concr. Res.* 28 (1998) 1023–1036.
- [5] M.H. Zhang, Effect of water-to-cementitious materials ratio and silica fume on the autogenous shrinkage of concrete, *Cem. Concr. Res.* 33 (2003) 1687–1694.
- [6] ACI Committee 116 R-85, Cement and concrete terminology, *ACI Manual of Concrete Practice*, American Concrete Institute pubs., USA, 1989.
- [7] M.D.A. Thomas, P.K. Mukherjee, The effect of slag on thermal cracking in concrete, in: R. Sprigenschmid (Ed.), *Thermal Cracking in Concrete at Early Ages*, 1994, pp. 197–204, Published.
- [8] R. Springenschmid, R. Breitenbucher, M. Mangold, Practical experience with concrete technology measures to avoid cracking, in: R. Sprigenschmid (Ed.), *Thermal Cracking in Concrete at Early Ages*, 1994, pp. 377–384, Published.
- [9] A.M. Alshamsi, Microsilica and granulated blast furnace slag effects on hydration temperature, *Cem. Concr. Res.* 27 (1997) 1851–1859.
- [10] Cengiz Duran Atis, Heat evolution of high-volume fly ash concrete, *Cem. Concr. Res.* 32 (2002) 751–756.
- [11] TU Chuanlin, JIN Shuangquan, LU Zhongming, Study on characteristics of RCC for Longtan Project, *J. Hydraul. Eng.* 4 (1999) 65–69 (in Chinese).
- [12] Ahmed Loukili, David Chopin, A new approach to determine autogenous shrinkage of mortar at an early age considering temperature history, *Cem. Concr. Res.* 30 (2000) 915–922.
- [13] Philippe Turcry, Ahmed Loukili, et al., Can the maturity concept be used to separate the autogenous shrinkage and thermal deformation of cement paste at early age? *Cem. Concr. Res.* 32 (2002) 1443–1450.
- [14] Lars Kraft, Hakan Engqvist, Leif Hermansson, Early-age deformation, drying shrinkage and thermal dilation in a new type of dental restorative material based on calcium aluminate cement, *Cem. Concr. Res.* 34 (2004) 439–446.
- [15] I. Shimasaki, K. Rokugo, H. Morimoto, Thermal expansion coefficient of concrete at very early age, in: Folker H. Wittmann, Hirozomihashi (Eds.), *Control of Cracking in Early Age Concrete*, 2000, pp. 29–36, Published.
- [16] T. Kawaguchi, Survey of published works on thermal expansion coefficient of mass concrete, *Proc. Of JCI Colloquium on thermal stress of Gifu National college of technology*, vol. JCI-C2, 1982, pp. 15–18.